
Proximal Iteration for Deep Reinforcement Learning

Kavosh Asadi¹ Rasool Fakoor¹ Omer Gottesman² Taesup Kim¹ Michael L. Littman² Alexander J. Smola¹

Abstract

We employ Proximal Iteration for value-function optimization in deep reinforcement learning. Proximal Iteration is a computationally efficient technique that enables biasing the optimization procedure towards desirable solutions. As a concrete application, we endow the objective function of Deep Q-Network (DQN) and Rainbow agents with a proximal term to ensure robustness in presence of large noise. The resultant agents, which we call DQN Pro and Rainbow Pro, exhibit significant improvements over their original counterparts on the Atari benchmark. Our results accentuate the power of employing sound optimization techniques for deep reinforcement learning.

1. Introduction

An important competency of reinforcement-learning (RL) agents is learning in environments with large state spaces like those found in robotics (Kober et al., 2013), dialog systems (Williams et al., 2017), and games (Tesauro, 1994; Silver et al., 2017). Recent breakthroughs in deep RL have demonstrated that simple approaches such as Q-learning (Watkins & Dayan, 1992) can surpass human-level performance in challenging environments when equipped with deep neural networks for function approximation (Mnih et al., 2015).

Two components of a gradient-based deep RL agent are its objective function and optimization procedure. The optimization procedure takes estimates of the gradient of the objective with respect to network parameters and updates the parameters accordingly. In DQN (Mnih et al., 2015), for example, the objective function is the empirical expectation of the temporal difference (TD) error (Sutton, 1988) on a buffered set of environmental interactions (Lin, 1992), and variants of stochastic gradient descent are employed to best minimize this objective function.

A fundamental difficulty in minimizing this objective func-

tion stems from the use of bootstrapping. In the context of RL, bootstrapping refers to the dependence of the target of gradient updates on the parameters of the neural network, which is itself continuously updated during training. Employing bootstrapping in RL stands in contrast to supervised-learning techniques and Monte-Carlo RL (Sutton & Barto, 2018), where the target of our gradient updates does not depend on the parameters of the neural network.

Mnih et al. (2015) proposed a simple and intriguing approach to hedging against issues that arise when using bootstrapping, specifically to use a *target network* in value-function optimization. In this case, the target network is updated periodically, and tracks the online network with some delay. While this modification constituted a major step towards combating misbehavior in Q-learning (Lee & He, 2019; Kim et al., 2019; Zhang et al., 2021), optimization instability is still prevalent (van Hasselt et al., 2018).

Our contribution is to employ Proximal Iteration for optimization in deep RL. By observing a synergy between DQN and Proximal Iteration (Ryu & Boyd, 2014), we endow the DQN and Rainbow (Hessel et al., 2018) agents with a proximal term that ensures the parameters of the online-network component remain in the vicinity of the parameters of the target network, thus increasing the robustness of RL to noisy updates. We present comprehensive experiments on the Atari benchmark (Bellemare et al., 2013), where the proximal agents yield significant improvements over their original counterparts, thus revealing the benefits of combining RL with Proximal Iteration.

2. Background and Notation

RL is the study of the interaction between an environment and an agent that learns to maximize reward through experience. The Markov Decision Process (Puterman, 1994), or MDP, is used to mathematically define the RL problem. An MDP is specified by the tuple $\langle \mathcal{S}, \mathcal{A}, \mathcal{R}, \mathcal{P}, \gamma \rangle$, where \mathcal{S} is the set of states and \mathcal{A} is the set of actions. The functions $\mathcal{R} : \mathcal{S} \times \mathcal{A} \rightarrow \mathbb{R}$ and $\mathcal{P} : \mathcal{S} \times \mathcal{A} \times \mathcal{S} \rightarrow [0, 1]$ denote the reward and transition dynamics of the MDP. Finally, by discounting future rewards, γ formalizes the intuitive notion that short-term rewards are more valuable than those received later.

¹Amazon Web Services ²Brown University. Correspondence to: Kavosh Asadi <kavasadi@amazon.com>.

The goal in the RL problem is to learn a policy, a mapping from states to a probability distribution over actions, $\pi : \mathcal{S} \rightarrow \mathcal{P}(\mathcal{A})$, that obtains high sums of future discounted rewards. An important concept in RL is the state value function. Formally, it denotes the expected discounted sum of future rewards when committing to a policy π in a state s :

$$v^\pi(s) := \mathbb{E} \left[\sum_{t=0}^{\infty} \gamma^t R_t \mid S_0 = s, \pi \right].$$

We define the Bellman operator \mathcal{T}^π as follows:

$$[\mathcal{T}^\pi v](s) := \sum_{a \in \mathcal{A}} \pi(a \mid s) (\mathcal{R}(s, a) + \sum_{s' \in \mathcal{S}} \gamma \mathcal{P}(s, a, s') v(s')),$$

which we write compactly as:

$$\mathcal{T}^\pi v := R^\pi + \gamma P^\pi v,$$

where $[R^\pi](s) = \sum_{a \in \mathcal{A}} \pi(a \mid s) \mathcal{R}(s, a)$ and $[P^\pi v](s) = \sum_{a \in \mathcal{A}} \pi(a \mid s) \sum_{s' \in \mathcal{S}} \mathcal{P}(s, a, s') v(s')$. We also denote:

$$(\mathcal{T}^\pi)^n v := \underbrace{\mathcal{T}^\pi \dots \mathcal{T}^\pi}_n v.$$

Notice that v^π is the unique fixed-point of $(\mathcal{T}^\pi)^n$ for all natural numbers n , meaning that $v^\pi = (\mathcal{T}^\pi)^n v^\pi$, for all n .

Define v^* as the optimal value of a state, namely: $v^*(s) := \max_\pi v^\pi(s)$, and π^* as a policy that achieves $v^*(s)$ for all states. We define the Bellman Optimality Operator \mathcal{T}^* :

$$[\mathcal{T}^* v](s) := \max_{a \in \mathcal{A}} \mathcal{R}(s, a) + \sum_{s' \in \mathcal{S}} \gamma \mathcal{P}(s, a, s') v(s'),$$

whose fixed point is v^* . These operators are at the heart of many planning and RL algorithms including Value Iteration (Bellman, 1957) and Policy Iteration (Howard, 1960).

3. Proximal Bellman Operator

In this section, we introduce a new class of Bellman operators that ensure that the next iterate in planning and RL remain in the proximity of the previous iterate.

To this end, we define the Bregman Divergence generated by a convex function f :

$$D_f(v', v) := f(v') - f(v) - \langle \nabla f(v), v' - v \rangle.$$

Examples include the l_p norm generated by $f(v) = \frac{1}{2} \|v\|_p^2$ and the Mahalanobis Distance generated by $f(v) = \frac{1}{2} \langle v, Qv \rangle$ for a positive semi-definite matrix Q .

We now define the Proximal Bellman Operator $(\mathcal{T}_{c,f}^\pi)^n$:

$$(\mathcal{T}_{c,f}^\pi)^n v := \arg \min_{v'} \|v' - (\mathcal{T}^\pi)^n v\|_2^2 + \frac{1}{c} D_f(v', v), \quad (1)$$

where $c \in (0, \infty]$. Intuitively, this operator encourages the next iterate to be in the proximity of the previous iterate, while also having a low error relative to the point recommended by the original Bellman Operator. The parameter c could, therefore, be thought of as a knob that controls the degree of gravitation towards the previous iterate.

Our goal is to understand the behavior of Proximal Bellman Operator when used in conjunction with the Modified Policy Iteration (MPI) algorithm (Puterman, 1994; Scherrer et al., 2015). Define $\mathcal{G}v$ as the greedy policy with respect to v . At a certain iteration k , Proximal Modified Policy Iteration (PMPI) proceeds as follows:

$$\pi_k \leftarrow \mathcal{G}v_{k-1}, \quad (2)$$

$$v_k \leftarrow (\mathcal{T}_{c,f}^{\pi_k})^n v_{k-1}. \quad (3)$$

The pair of updates above generalize existing algorithms. Notably, with $c \rightarrow \infty$ and general n we get MPI, with $c \rightarrow \infty$ and $n = 1$ the algorithm reduces to Value Iteration, and with $c \rightarrow \infty$ and $n = \infty$ we have a reduction to Policy Iteration. For finite c , the two extremes of n , namely $n = 1$ and $n = \infty$, could be thought of as the proximal versions of Value Iteration and Policy Iteration, respectively.

To analyze this approach, it is first natural to ask if each iteration of PMPI could be thought of as a contraction so we can get sound and convergent behavior in planning and learning. For $n > 1$, Scherrer et al. (2015) constructed a contrived MDP demonstrating that one iteration of MPI can unfortunately expand. As PMPI is just a generalization of MPI, the same example from Scherrer et al. (2015) shows that PMPI can expand. In the case of $n = 1$, we can rewrite the pair of equations (2) and (3) in a single update as follows:

$$v_k \leftarrow \mathcal{T}_{c,f}^* v_{k-1}.$$

When $c \rightarrow \infty$, standard proofs can be employed to show that the operator is a contraction (Littman & Szepesvári, 1996). We now show that $\mathcal{T}_{c,f}^*$ is a contraction for finite values of c . See our appendix for proofs.

Theorem 1. *The Proximal Bellman Optimality Operator $\mathcal{T}_{c,f}^*$ is a contraction with fixed point v^* .*

Therefore, we get convergent behavior when using $\mathcal{T}_{c,f}^*$ in planning and RL. The addition of the proximal term is fortunately not changing the fixed point, thus not negatively affecting the final solution. This could be thought of as a form of regularization that vanishes in the limit; the algorithm converges to v^* even without decaying $1/c$.

Going back to the general $n \geq 1$ case, following previous work (Bertsekas & Tsitsiklis, 1996; Scherrer et al., 2015), we study PMPI in presence of additive noise where we get a noisy sample of the original Bellman Operator $(\mathcal{T}^{\pi_k})^n v_{k-1} + \epsilon_k$. The noise can stem from a variety of reasons, such as function approximation or sampling error.

For simplicity, we restrict the analysis to the case where $D_f(v', v) = \|v' - v\|_2^2$, so we can simply write update (3) in PMPI as:

$$v_k \leftarrow \arg \min_{v'} \|v' - ((\mathcal{T}^{\pi_k})^n v_{k-1} + \epsilon_k)\|_2^2 + \frac{1}{c} \|v' - v_{k-1}\|_2^2$$

which can further be simplified to:

$$v_k \leftarrow \underbrace{(1 - \beta)(\mathcal{T}^{\pi_k})^n v_{k-1} + \beta v_{k-1}}_{:= (\mathcal{T}_\beta^{\pi_k})^n v_{k-1}} + (1 - \beta)\epsilon_k,$$

where $\beta = \frac{1}{1+c}$. This operator is a generalization of the operator proposed by [Smirnova & Dohmatob \(2020\)](#) who focused on the case of $n = 1$. To build some intuition, notice that the update is multiplying error ϵ_k by a term that is smaller than one, thus better hedging against large noise. While the update may slow progress when there is no noise, it is entirely conceivable that for large enough values of ϵ_k , it is better to use non-zero β values. In the following theorem we formalize this intuition. Our result leans on the theory provided by [Scherrer et al. \(2015\)](#) and could be thought of as a generalization of their theorem for non-zero β values.

Theorem 2. *Consider the PMPI algorithm specified by:*

$$\pi_k \leftarrow \mathcal{G}_{\epsilon'_k} v_{k-1}, \quad (4)$$

$$v_k \leftarrow (\mathcal{T}_\beta^{\pi_k})^n v_{k-1} + (1 - \beta)\epsilon_k. \quad (5)$$

Define the Bellman residual $b_k := v_k - \mathcal{T}^{\pi_{k+1}} v_k$, and error terms $x_k := (I - \gamma P^{\pi_k})\epsilon_k$ and $y_k := \gamma P^{\pi^*} \epsilon_k$. After k steps:

$$v^* - v^{\pi_k} = \underbrace{v^{\pi^*} - (\mathcal{T}_\beta^{\pi_{k+1}})^n v_k}_{d_k} + \underbrace{(\mathcal{T}_\beta^{\pi_{k+1}})^n v_k - v_{\pi_k}}_{s_k}$$

- where $d_k \leq \gamma P^{\pi^*} d_{k-1} - ((1 - \beta)y_{k-1} + \beta b_{k-1}) + (1 - \beta) \sum_{j=1}^{n-1} (\gamma P^{\pi_k})^j b_{k-1} + \epsilon'_k$
- $s_k \leq ((1 - \beta)(\gamma P^{\pi_k})^n + \beta I)(I - \gamma P^{\pi_k})^{-1} b_{k-1}$
- $b_k \leq ((1 - \beta)(\gamma P^{\pi_k})^n + \beta I) b_{k-1} + (1 - \beta)x_k + \epsilon'_{k+1}$

The bound provides intuition as to how the proximal Bellman Operator can accelerate convergence in the presence of high noise. For simplicity, we will only analyze the effect of the ϵ noise term, and ignore the ϵ' term. We first look at the Bellman residual, b_k . Given the Bellman residual in iteration $k - 1$, b_{k-1} , the only influence of the noise term ϵ_k on b_k is through the $(1 - \beta)x_k$, term, and we see that b_k decreases linearly with larger β .

The analysis of s_k is slightly more involved but follows similar logic. The bound for s_k can be decomposed into a term proportional to b_{k-1} and a term proportional to βb_{k-1} ,

where both are multiplied with positive semi-definite matrices. Since b_{k-1} itself linearly decreases with β , we conclude that larger β decreases the bound quadratically.

The effect of β on the bound for d_k is more complex. The terms βy_{k-1} and $\sum_{j=1}^{n-1} (\gamma P^{\pi_k})^j b_{k-1}$ introduce a linear decrease of the bound on d_k with β , while the term $\beta(I - \sum_{j=1}^{n-1} (\gamma P^{\pi_k})^j) b_{k-1}$ introduces a quadratic dependence whose curvature depends on $I - \sum_{j=1}^{n-1} (\gamma P^{\pi_k})^j$. This complex dependence on β highlights the trade-off between noise reduction and magnitude of updates. To understand this trade-off better, we examine two extreme cases for the magnitude on the noise. When the noise is very large, we may set $\beta = 1$, equivalent to an infinitely strong proximal term. It is easy to see that for $\beta = 1$, the values of d_k and s_k remain unchanged, which is preferable to the increase they would suffer in the presence of very large noise. On the other extreme, when no noise is present, the x_k and y_k terms in [Theorem 2](#) vanish, and the bounds on d_k and s_k can be minimized by setting $\beta = 0$, i.e. without noise the proximal term should not be used and the original Bellman update performed. Intermediate noise magnitudes thus require a value of β that balances the noise reduction and update size.

4. Deep Q-Network with Proximal Iteration

Leveraging the insights we built in the previous section, we now endow the DQN-style family of algorithms with a proximal term. To this end, consider the following optimization problem:

$$\min_w h(x; w), \quad (6)$$

where h is the objective function (for example, the TD error), w denotes the learnable parameters (the parameters of a Q-network), and x is the input data ($\langle s, a, r, s' \rangle$). For ease of presentation, we write $h(x; w)$ as $h(w)$. If h is differentiable, then Stochastic Gradient Descent (SGD), which proceeds as follows:

$$w_k \leftarrow w_{k-1} - \alpha_k \nabla_w h(w_{k-1}), \quad k = 1, 2, 3, \dots \quad (7)$$

could be used to solve the optimization problem (6). Here, α_k denotes the step size at iteration k , and w_0 is an arbitrary starting point.

While SGD is well-behaved asymptotically and under standard assumptions, it can perform recklessly in the interim, leading into a situation where the iterates get exponentially far from the solution ([Moulines & Bach, 2011](#); [Ryu & Boyd, 2014](#)). This behavior can be particularly harmful in the context of RL where stability is an important concern.

A simple approach to stabilizing SGD is to augment the objective with a quadratic regularizer to ensure that each iterate stays in the vicinity of the previous one:

$$w_k = \arg \min_w h(w) + \frac{1}{2c} \|w - w_{k-1}\|_2^2. \quad (8)$$

Notice that the parameter \tilde{c} plays a role analogous to that of the parameter c in the Proximal Bellman Operator (1).

Having completed iteration k , we replace the previous iterate w_{k-1} by its new value w_k and then proceed to iteration $k + 1$.

While the asymptotic performance of SGD and Proximal Iteration are analogous (Ryu & Boyd, 2014), they may exhibit qualitatively different behavior *en route*. More concretely, denote the stepsize of SGD and Proximal Iteration at iteration k by $\alpha_k = \frac{D}{k}$, and $w^* := \arg \min_w h(w)$. Under standard assumptions, for SGD we have (Bauschke & Combettes, 2011):

$$\mathbb{E} [\|w_k - w^*\|_2^2] \leq \mathcal{O} \left(\frac{\exp(D^2)}{k^D} + \frac{1}{k} \right).$$

The exponential dependence on D^2 can indeed occur as Ryu & Boyd (2014) demonstrate via an example. In contrast, for Proximal Iteration we have (Ryu & Boyd, 2014):

$$\mathbb{E} [\|w_k - w^*\|_2^2] \leq \|w_0 - w^*\|_2^2 + \sum_{i=1}^k \alpha_i.$$

Therefore, Proximal Iteration is fairly well-behaved in the interim.

We now incorporate this proximal term for value-function optimization into deep RL. For clarity, we focus on the original DQN, but the derivation is similar for advanced variants of DQN like Rainbow.

Recall that DQN employs two parameterized value functions: an online network $\hat{Q}(s, a; w)$ that is updated at each step, and a target network $\hat{Q}(s, a; \theta)$ that is used for bootstrapping and is synchronized with the online network periodically. Let tuples $\langle s, a, r, s' \rangle$ denote the buffered environmental interactions of the RL agent. Define the following objective function like that used in DQN:

$$h(w) := \widehat{\mathbb{E}}_{\langle s, a, r, s' \rangle} \left[\left(r + \gamma \max_{a'} \hat{Q}(s', a'; \theta) - \hat{Q}(s, a; w) \right)^2 \right]. \quad (9)$$

Our desire is to find a setting of weights w that minimizes h . We can do so by applying SGD, but, as argued above, it can lead to reckless updates. As a hedge, we bias the online weights towards the previous iterate. The target network is a natural choice for this purpose, motivating the following objective:

$$\arg \min_w h(w) + \frac{1}{2\tilde{c}} \|w - \theta\|_2^2.$$

To solve this minimization problem, we can take multiple descent steps using the stochastic gradients of the objective.

Thus, starting from the initial point $w = \theta$, we perform multiple w updates (specified by the *period* hyper-parameter):

$$\begin{aligned} w &= \theta \\ \text{for } i = 1 \dots \text{period:} \\ w &\leftarrow w - \alpha (\nabla h(w) + \frac{1}{\tilde{c}} (w - \theta)) \\ \theta &\leftarrow w. \end{aligned} \quad (10)$$

In the last step, akin to the original DQN, we synchronize the two networks by performing $\theta \leftarrow w$, before moving to the subsequent iteration. This iterative optimization proceeds until convergence is obtained.

Observe that the online-network update (10) can equivalently be written as:

$$w \leftarrow (1 - (\alpha/\tilde{c})) \cdot w + (\alpha/\tilde{c}) \cdot \theta - \alpha \nabla h(w). \quad (11)$$

Notice the intuitively appealing form of the update: we first compute a convex combination of θ and w , based on the hyper-parameters α and \tilde{c} , then add the gradient term to arrive at the next iterate of w . If w and θ are close, the convex combination is close to w itself and so this *DQN Pro* update would in effect perform an update similar to that of the original DQN. However, when the online weight w strays too far from the previous target-network iterate, taking the convex combination ensures that the online network gravitates towards the target network by default. In other words, the gradient signal from minimizing the squared TD error (9) needs to be strong enough to compensate for the default gravitation towards θ . The update includes the original DQN update as a special case when $\tilde{c} \rightarrow \infty$.

The pseudo-code for DQN Pro is presented in Algorithm 1. The difference between DQN (Mnih et al., 2015) and our DQN Pro is minimal, and is highlighted in red. Note that DQN Pro adds negligible computational cost to DQN. While the particular form of DQN Pro presented in Algorithm 1 uses SGD as the optimizer, the idea can be used in conjunction with other optimizers such as Adam (Kingma & Ba, 2015).

5. Experiments

In this section, we empirically investigate the effectiveness of introducing the proximal term to planning and reinforcement-learning algorithms. We begin by conducting experiments with PMPI in the context of approximate planning, and then move to large-scale RL experiments in Atari.

5.1. PMPI Experiments

We now focus on understanding the empirical impact of adding the proximal term on the performance of approxi-

Algorithm 1 DQN with Proximal Iteration (DQN Pro)

```

1: Initialize  $\theta$ ,  $N$ , period, replay buffer  $\mathcal{D}$ ,  $\alpha$ , and  $\tilde{c}$ 
2:  $s \leftarrow \text{env.reset}()$ ,  $w \leftarrow \theta$ ,  $\text{numUpdates} \leftarrow 0$ 
3: repeat
4:    $a \sim \epsilon\text{-greedy}(Q(s, \cdot; w))$ 
5:    $s', r \leftarrow \text{env.step}(s, a)$ 
6:   add  $\langle s, a, r, s' \rangle$  to  $\mathcal{D}$ 
7:   if  $s'$  is terminal then
8:      $s \leftarrow \text{env.reset}()$ 
9:   end if
10:  for  $n$  in  $\{1, \dots, N\}$  do
11:    sample a batch  $\mathcal{B} = \{\langle s, a, r, s' \rangle\}$  from  $\mathcal{D}$  and
    compute  $\nabla_w h(w)$ 
12:     $w \leftarrow (1 - (\alpha/\tilde{c}))w + (\alpha/\tilde{c})\theta - \alpha \nabla_w h(w)$ 
13:     $\text{numUpdates} \leftarrow \text{numUpdates} + 1$ 
14:    if  $\text{numUpdates} \% \text{period} = 0$  then
15:       $\theta \leftarrow w$ 
16:    end if
17:  end for
18: until convergence
    
```

mate PMPI. To this end, we use the pair of update equations:

$$\begin{aligned} \pi_k &\leftarrow \mathcal{G}v_{k-1}, \\ v_k &\leftarrow (1 - \beta)((\mathcal{T}^{\pi_k})^n v_{k-1} + \epsilon_k) + \beta v_{k-1}. \end{aligned}$$

For this experiment, we chose the toy 8×8 Frozen Lake environment from Open AI Gym (Brockman et al., 2016), where the transition and reward model of the environment is available to the planner. Using a small environment allows us to understand the impact of the proximal term in the simplest and most clear setting. Note also that we arranged the experiment so that the policy greedification step $\mathcal{G}v_{k-1} \forall k$ is error-free, so we can solely focus on the interplay between the proximal term and the error caused by imperfect policy evaluation.

We applied 100 iterations of PMPI, then measured the quality of the resultant policy $\pi := \pi_{100}$ as defined by the distance between its true value and that of the optimal policy, namely $\|V^* - V^\pi\|_\infty$. We repeated the experiment with different magnitudes of error, as well as different values of the β parameter.

From Figure 1, it is clear that the final performance exhibits a U-shape with respect to the parameter β . It is also noticeable that the best-performing β is shifting to the right side (larger values) as we increase the magnitude of noise. This trend makes sense, and is consistent with what is predicted by Theorem 2: As the noise level rises, we have more incentive to use larger (but not too large) β values to hedge against it.

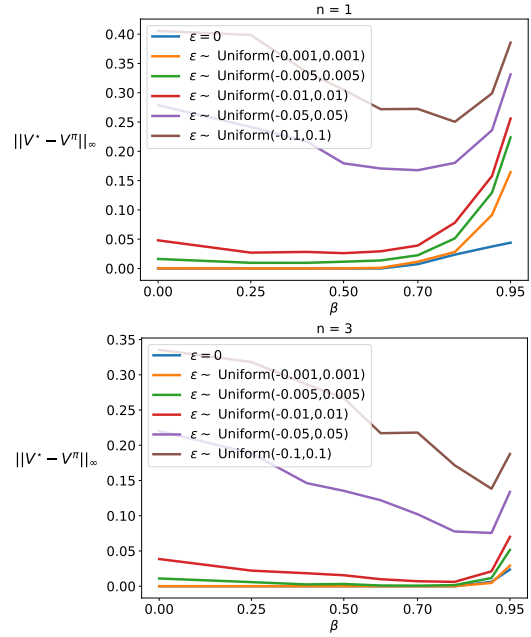


Figure 1. Performance of approximate PMPI has a U-shaped dependence on the parameter $\beta = \frac{1}{1+c}$. Results are averaged over 30 random seeds with $n = 1$ (top) and $n = 3$ (bottom).

5.2. Atari Experiments

In this section, we evaluate the proximal (or Pro) agents relative to their original DQN-style counterparts on the Atari benchmark (Bellemare et al., 2013), and show that endowing the agent with the proximal term can lead into significant improvements in the interim as well as in the final performance. We next investigate the utility of our proposed proximal term through further experiments. Please see the Appendix for a complete description of our experimental pipeline.

5.2.1. SETUP

We used 55 Atari games (Bellemare et al., 2013) to conduct our experimental evaluations. Following Machado et al. (2018) and Castro et al. (2018), we used sticky actions to inject stochasticity into the otherwise deterministic Atari emulator.

Our training and evaluation protocols and the hyperparameter settings closely follow those of the Dopamine baseline (Castro et al., 2018), which is consistent with the existing literature. To report performance, we measured the undiscounted sum of rewards obtained by the learned policy during evaluation. We further report the learning curve for all experiments averaged across 5 random seeds. We reiterate that we used the same network architecture as that of Mnih et al. (2015) for all experiments in this paper and we also used the exact same hyper-parameters for all agents to ensure a sound comparison. Our Pro agents re-

quire a single additional hyper-parameter, namely \tilde{c} . We did a minimal random search to tune this value. Then, for each Pro agent, we used the same \tilde{c} value across all games. More details are provided in the Appendix.

5.2.2. RESULTS

The most important question is whether endowing the DQN agent with the proximal term can yield significant improvements over the original DQN. To answer this question in the affirmative, our first result is a large-scale comparison between DQN and DQN Pro. Figure 2 (top) shows a comparison between DQN and DQN Pro in terms of the final performance. In particular, following standard practice (Wang et al., 2016; Dabney et al., 2018; van Seijen et al., 2019), for each game we compute:

$$\frac{\text{Score}_{\text{DQN Pro}} - \text{Score}_{\text{DQN}}}{\max(\text{Score}_{\text{DQN}}, \text{Score}_{\text{Human}}) - \text{Score}_{\text{Random}}}.$$

Bars shown in red indicate the games in which we observed better final performance for DQN Pro relative to DQN, and bars in blue indicate the opposite. The height of a bar denotes the magnitude of this improvement for the corresponding benchmark; notice that the y-axis is scaled logarithmically. We took human and random scores from previous work (Nair et al., 2015; Dabney et al., 2018).

It is clear that DQN Pro dramatically improves upon DQN. This improvement is particularly rewarding in light of the fact that the implementation of DQN Pro is just minimally different than that of DQN, and that DQN Pro adds almost no additional computational burden to the original DQN agent. We defer to the Appendix for full learning curves on all games tested.

Can we fruitfully combine the benefits offered by the proximal term with some of the existing algorithmic improvements in DQN? To answer this question, we focus on the work of Hessel et al. (2018) who successfully combined numerous important algorithmic ideas in the value-based RL literature, resulting in an algorithm called Rainbow that demonstrated impressive improvements over the state-of-the-art. Our hypothesis was that adding the proximal term to Rainbow will offer additional improvements in light of the fact that the proximal term is addressing a qualitatively different problem than the existing components of Rainbow do. To test this hypothesis, we compared the performance of Rainbow Pro versus Rainbow on the same games from the previous experiment. We present this result in Figure 2 (bottom). Observe that the overall trend is for Rainbow Pro to yield large performance improvements over Rainbow.

Additionally, we measured the performance of our agents relative to human players. Measuring this quantity has been an inspiration for researchers to introduce algorithmic improvements since the introduction of DQN. To this end, and

again following previous work (Wang et al., 2016; Dabney et al., 2018; van Seijen et al., 2019), for each agent we compute the human-normalized score:

$$\frac{\text{Score}_{\text{Agent}} - \text{Score}_{\text{Random}}}{\text{Score}_{\text{Human}} - \text{Score}_{\text{Random}}}.$$

In Figure 3, we show the median of this score for all agents, which Wang et al. (2016) and Hessel et al. (2018) argued is a sensible quantity to track.

We make two key observations from this figure. First, the original DQN Pro agent, which is relatively simple to understand and implement, is capable of achieving human-level performance (1.0 on the y-axis) after 120 million frames. Second, the Rainbow Pro agent achieves 220 percent human-normalized score after only 120 million frames.

5.2.3. ADDITIONAL EXPERIMENTS

Our purpose in endowing the agent with the proximal term was to keep the online network in the vicinity of the target network, so it would be natural to ask if this desirable property can manifest itself in practice when using the proximal term. In Figure 4, we answer this question affirmatively by plotting the magnitude of the update to the target network during synchronization. Notice that we periodically synchronize online and target networks, so the proximity of the online and target network should manifest itself in a low distance between two consecutive target networks. Indeed, the results demonstrate the success of the proximal term in terms of obtaining the desired proximity of online and target networks.

While using the proximal term leads to significant improvements, one may still wonder if the advantage of DQN Pro over DQN is merely stemming from a poorly-chosen *period* hyper-parameter in the original DQN, as opposed to a truly more stable optimization in DQN Pro. To refute this hypothesis, we ran DQN with various settings of the *period* hyper-parameter $\{2000, 4000, 8000, 12000\}$. This set included the default value of the hyper-parameter (8000) from the original paper (Mnih et al., 2015), but also covered a wider set of settings.

Additionally, we tried an alternative update strategy for the target network, referred to as Polyak averaging, which was popularized in the context of continuous-action RL (Lillicrap et al., 2015), and which proceeds by updating the target network as follows: $\theta \leftarrow \tau w + (1 - \tau)\theta$. For this update strategy, too, we tried different settings of the τ hyper-parameter, namely $\{0.05, 0.005, 0.0005\}$, which includes the value 0.005 used in numerous papers (Lillicrap et al., 2015; Fujimoto et al., 2018; Asadi et al., 2021).

Figures 5 and 6 present a comparison between DQN Pro and DQN with periodic and Polyak target updates for various hyper-parameter settings of *period* and τ . It is clear

Proximal Iteration for Deep Reinforcement Lefarning

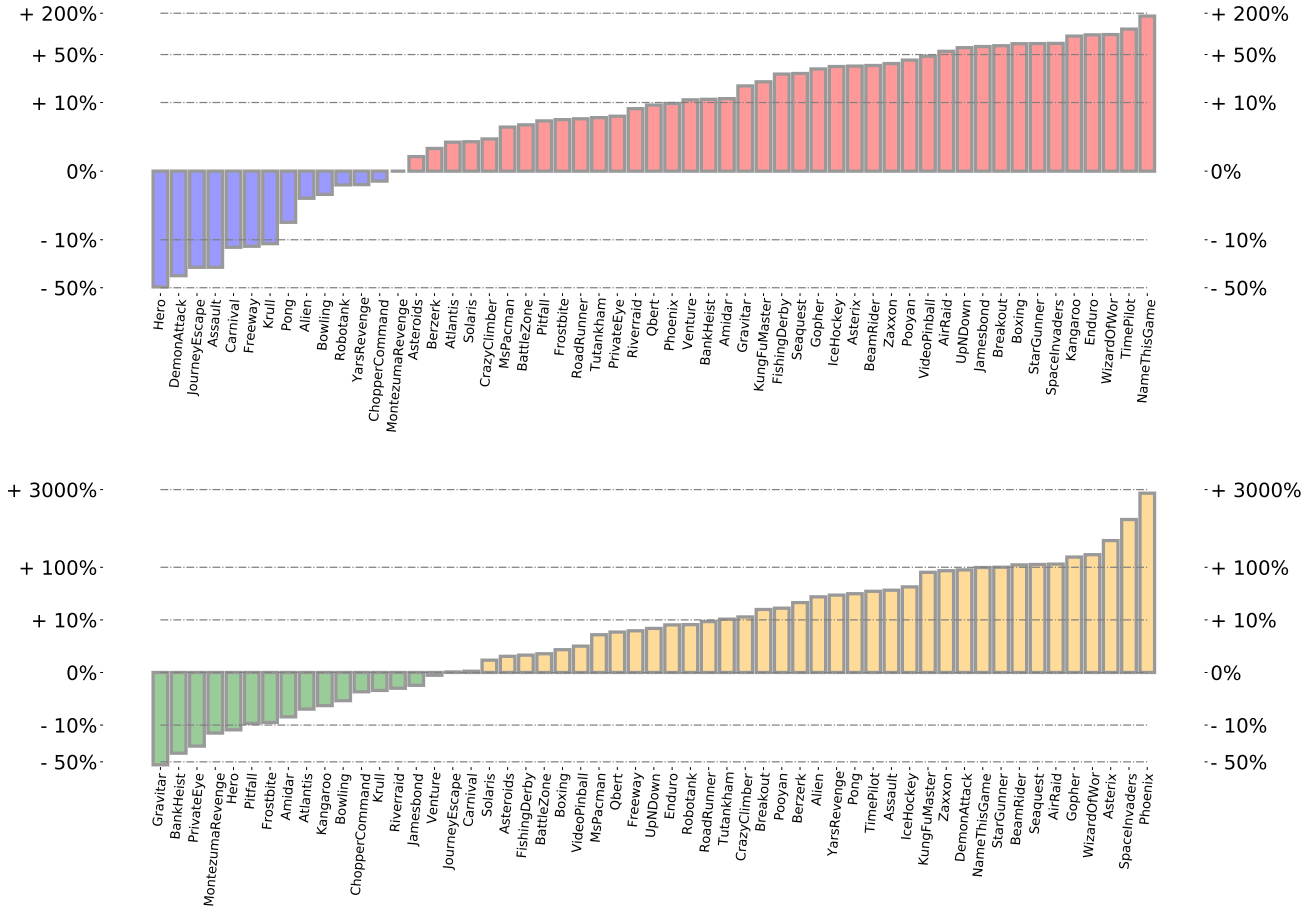


Figure 2. Final gain for DQN Pro over DQN (top), and Rainbow Pro over Rainbow (bottom). Results are averaged over 5 random seeds, and the Y-axis is scaled logarithmically. DQN Pro and Rainbow Pro significantly outperform their original counterparts.

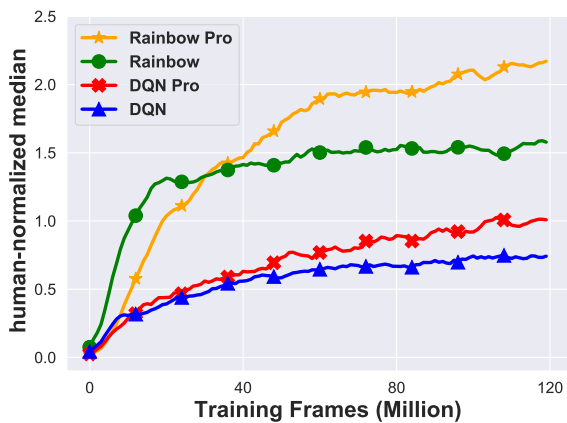


Figure 3. The learning curve for DQN, Rainbow and their “Pro” counterparts in terms of median human-normalized score. Results are averaged over 5 random seeds. The Pro agents yield significant improvements.

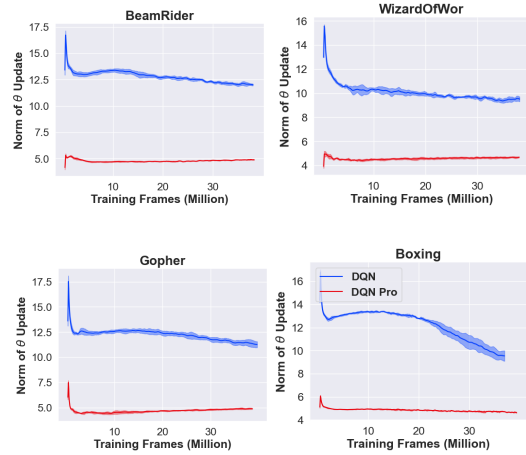


Figure 4. Using the proximal term reduces the magnitude of target network updates.

that DQN Pro is consistently outperforming the two alternatives regardless of the specific values of $period$ and τ , thus clearly demonstrating that the improvement is stemming from a more stable optimization procedure leading to a better interplay between the two networks.

We also note that in our experience working with the proximal term in the parameter space was superior than doing so in the value space. We believe this is because the parameter-space definition can enforce the proximity globally, while in the value space one can only hope to obtain proximity locally and on the batch of samples drawn from the experience-replay buffer.

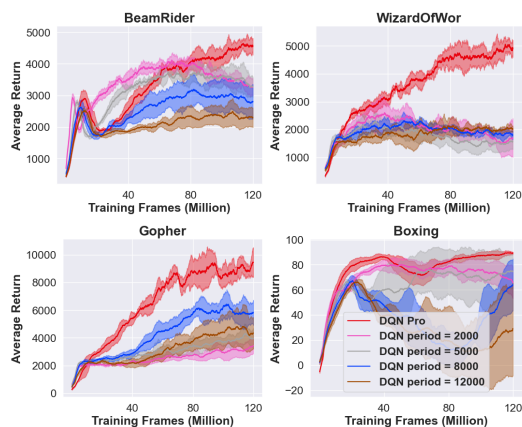


Figure 5. A comparison between DQN Pro and DQN with periodic updates for target network.



Figure 6. A comparison between DQN Pro and DQN with Polyak updates for target network.

6. Related Work

The introduction of proximal operators could be traced back to the seminal work of Moreau (1962; 1965), Mar-

tinet (1970) and Rockafellar (1976), and the use of the proximal operators has since expanded into many areas of science such as signal processing (Combettes & Pesquet, 2009), statistics and machine learning (Beck & Teboulle, 2009; Polson et al., 2015; Reddi et al., 2015), and convex optimization (Parikh & Boyd, 2014; Bertsekas, 2011b;a).

In the context of RL, Mahadevan et al. (2014) introduced a proximal theory for deriving convergent off-policy algorithms with linear function approximation. One intriguing characteristic of their work is that they perform updates in primal-dual space, a property that was leveraged in sample complexity analysis (Liu et al., 2020) for the proximal counterparts of the gradient temporal-difference algorithm (Sutton et al., 2008). Proximal operators also have appeared in the deep RL literature. For instance, Fakoor et al. (2020b) used proximal operators for meta learning, and Maggipinto et al. (2020) improved TD3 (Fujimoto et al., 2018) by employing a stochastic proximal-point interpretation.

The effect of the proximal term in our work is reminiscent of the use of trust regions in policy-gradient algorithms (Schulman et al., 2015; 2017; Wang et al., 2019; Fakoor et al., 2020a; Tomar et al., 2021). However, three factors differentiate our work: we define the proximal term using the value function, not the policy, we enforce the proximal term in the parameter space, as opposed to the function space, and we use the target network as the previous iterate in our proximal definition.

Finally, existing work in RL showed the benefits of leveraging the structure of the RL problem during optimization. For example, Precup & Sutton (1997) argued that the space of value functions could better be understood as a manifold with an entropic metric, resulting in the exponentiated TD algorithm. Mahadevan & Liu (2012) used mirror descent to penalize weights with large p-norms. Similarly, van Seijen et al. (2019) advocated for performing Q-updates in a logarithmic space to combat issues that arise in problems where the action-gap (Farahmand, 2011) can vary drastically on a state-by-state basis.

7. Conclusion and Future work

We showed a clear advantage for using proximal terms in approximate planning and reinforcement learning. More specifically, using a proximal term in DQN ensures that the online network remains in the vicinity of the target network, leading to robustness with respect to noise. Several improvements to proximal methods exist, such as the acceleration algorithm (Nesterov, 1983; Li & Lin, 2015), as well as using other proximal terms (Combettes & Pesquet, 2009), which we leave for future work. More generally, our results demonstrate the rewarding nature of developing principled optimization techniques for deep reinforcement learning.

8. Acknowledgements

The authors gratefully acknowledge the assistance of George D. Konidaris, Lihong Li, Cameron Allen, Sina Ghiassian, and Martin Klissarov.

References

- Asadi, K., Parikh, N., Parr, R. E., Konidaris, G. D., and Littman, M. L. Deep radial-basis value functions for continuous control. In AAAI Conference on Artificial Intelligence, 2021.
- Bauschke, H. H. and Combettes, P. L. Convex analysis and monotone operator theory in Hilbert spaces. 2011.
- Beck, A. and Teboulle, M. A fast iterative shrinkage-thresholding algorithm for linear inverse problems. SIAM Journal on Imaging Sciences, 2009.
- Bellemare, M. G., Naddaf, Y., Veness, J., and Bowling, M. The arcade learning environment: An evaluation platform for general agents. Journal of Artificial Intelligence Research, 2013.
- Bellman, R. E. Dynamic Programming. 1957.
- Bertsekas, D. P. Incremental gradient, subgradient, and proximal methods for convex optimization: A survey. Optimization for Machine Learning, 2011a.
- Bertsekas, D. P. Incremental proximal methods for large scale convex optimization. Mathematical Programming, 2011b.
- Bertsekas, D. P. and Tsitsiklis, J. N. Neuro-dynamic programming. Athena Scientific, 1996.
- Brockman, G., Cheung, V., Pettersson, L., Schneider, J., Schulman, J., Tang, J., and Zaremba, W. Openai gym, 2016.
- Castro, P. S., Moitra, S., Gelada, C., Kumar, S., and Bellemare, M. G. Dopamine: A Research Framework for Deep Reinforcement Learning. 2018.
- Combettes, P. L. and Pesquet, J.-C. Proximal Splitting Methods in Signal Processing. Fixed-point algorithms for inverse problems in science and engineering, 2009.
- Dabney, W., Ostrovski, G., Silver, D., and Munos, R. Implicit quantile networks for distributional reinforcement learning. In International conference on machine learning, pp. 1096–1105. PMLR, 2018.
- Fakoor, R., Chaudhari, P., and Smola, A. J. P3O: Policy-on policy-off policy optimization. In Conference on Uncertainty in Artificial Intelligence, 2020a.
- Fakoor, R., Chaudhari, P., Soatto, S., and Smola, A. J. Meta-Q-learning. In International Conference on Learning Representations, 2020b.
- Farahmand, A. Action-gap phenomenon in reinforcement learning. Advances in Neural Information Processing Systems, 2011.
- Fujimoto, S., Hoof, H., and Meger, D. Addressing function approximation error in actor-critic methods. In International Conference on Machine Learning, 2018.
- Hessel, M., Modayil, J., van Hasselt, H., Schaul, T., Ostrovski, G., Dabney, W., Horgan, D., Piot, B., Azar, M., and Silver, D. Rainbow: Combining improvements in deep reinforcement learning. In AAAI Conference on Artificial Intelligence, 2018.
- Howard, R. A. Dynamic programming and markov processes. 1960.
- Kim, S., Asadi, K., Littman, M., and Konidaris, G. Deepmellow: removing the need for a target network in deep q-learning. In International Joint Conference on Artificial Intelligence, 2019.
- Kingma, D. P. and Ba, J. Adam: A method for stochastic optimization. In International Conference on Learning Representations, 2015.
- Kober, J., Bagnell, J. A., and Peters, J. Reinforcement learning in robotics: A survey. International Journal of Robotics Research, 2013.
- Lee, D. and He, N. Target-based temporal-difference learning. In International Conference on Machine Learning, 2019.
- Li, H. and Lin, Z. Accelerated proximal gradient methods for nonconvex programming. Advances in neural information processing systems, 2015.
- Lillicrap, T. P., Hunt, J. J., Pritzel, A., Heess, N., Erez, T., Tassa, Y., Silver, D., and Wierstra, D. Continuous control with deep reinforcement learning. In International Conference on Learning Representations, 2015.
- Lin, L.-J. Self-improving reactive agents based on reinforcement learning, planning and teaching. Machine learning, 1992.
- Littman, M. L. and Szepesvári, C. A generalized reinforcement-learning model: Convergence and applications. In ICML, volume 96, pp. 310–318. Citeseer, 1996.
- Liu, B., Liu, J., Ghavamzadeh, M., Mahadevan, S., and Petrik, M. Finite-sample analysis of proximal gradient TD algorithms. In Conference on Uncertainty in Artificial Intelligence, 2020.

- Machado, M. C., Bellemare, M. G., Talvitie, E., Veness, J., Hausknecht, M., and Bowling, M. Revisiting the arcade learning environment: Evaluation protocols and open problems for general agents. Journal of Artificial Intelligence Research, 2018.
- Maggipinto, M., Susto, G. A., and Chaudhari, P. Proximal deterministic policy gradient. In International Conference on Intelligent Robots and Systems, 2020.
- Mahadevan, S. and Liu, B. Sparse q-learning with mirror descent. In Conference on Uncertainty in Artificial Intelligence, 2012.
- Mahadevan, S., Liu, B., Thomas, P., Dabney, W., Giguere, S., Jacek, N., Gemp, I., and Liu, J. Proximal Reinforcement Learning: A New Theory of Sequential Decision Making in Primal-Dual Spaces. arXiv, 2014.
- Martinet, B. Regularisation, d'inéquations variationnelles par approximations successives. Revue Française d'informatique et de Recherche operationelle, 1970.
- Mnih, V., Kavukcuoglu, K., Silver, D., Rusu, A. A., Veness, J., Bellemare, M. G., Graves, A., Riedmiller, M., Fidjeland, A. K., Ostrovski, G., et al. Human-level control through deep reinforcement learning. Nature, 2015.
- Moreau, J. J. Fonctions convexes duales et points proximaux dans un espace hilbertien. Comptes rendus hebdomadaires des séances de l'Académie des sciences, 1962.
- Moreau, J. J. Proximité et dualité dans un espace hilbertien. Bulletin de la Société Mathématique de France, 1965.
- Moulines, E. and Bach, F. Non-asymptotic analysis of stochastic approximation algorithms for machine learning. In Advances in Neural Information Processing Systems, 2011.
- Nair, A., Srinivasan, P., Blackwell, S., Alcicek, C., Fearon, R., De Maria, A., Panneershelvam, V., Suleyman, M., Beattie, C., Petersen, S., et al. Massively parallel methods for deep reinforcement learning. arXiv preprint arXiv:1507.04296, 2015.
- Nesterov, Y. A method for unconstrained convex minimization problem with the rate of convergence $O(1/k^2)$. In Doklady an USSR, 1983.
- Parikh, N. and Boyd, S. proximal algorithms. Foundations and Trends in optimization, 2014.
- Polson, N. G., Scott, J. G., and Willard, B. T. Proximal algorithms in statistics and machine learning. Statistical Science, 2015.
- Precup, D. and Sutton, R. S. Exponentiated gradient methods for reinforcement learning. In International Conference on Machine Learning, 1997.
- Puterman, M. L. Markov Decision Processes: Discrete Stochastic Dynamic Programming. 1994.
- Reddi, S., Póczos, B., and Smola, A. Doubly robust covariate shift correction. In AAAI Conference on Artificial Intelligence, 2015.
- Rockafellar, R. T. Monotone operators and the proximal point algorithm. SIAM Journal on Control and Optimization, 1976.
- Ryu, E. K. and Boyd, S. Stochastic proximal iteration: a non-asymptotic improvement upon stochastic gradient descent. 2014.
- Scherrer, B., Ghavamzadeh, M., Gabillon, V., Lesner, B., and Geist, M. Approximate modified policy iteration and its application to the game of tetris. J. Mach. Learn. Res., 16:1629–1676, 2015.
- Schulman, J., Levine, S., Abbeel, P., Jordan, M., and Moritz, P. Trust region policy optimization. In International conference on machine learning, 2015.
- Schulman, J., Wolski, F., Dhariwal, P., Radford, A., and Klimov, O. Proximal policy optimization algorithms. arXiv, 2017.
- Silver, D., Schrittwieser, J., Simonyan, K., Antonoglou, I., Huang, A., Guez, A., Hubert, T., Baker, L., Lai, M., Bolton, A., et al. Mastering the game of go without human knowledge. Nature, 2017.
- Smirnova, E. and Dohmatob, E. On the convergence of smooth regularized approximate value iteration schemes. Advances in Neural Information Processing Systems, 33, 2020.
- Sutton, R. S. Learning to predict by the methods of temporal differences. Machine learning, 1988.
- Sutton, R. S. and Barto, A. G. Reinforcement learning: An introduction. 2018.
- Sutton, R. S., Szepesvári, C., and Maei, H. R. A convergent $O(n)$ temporal-difference algorithm for off-policy learning with linear function approximation. In Advances in Neural Information Processing Systems, 2008.
- Tesauro, G. TD-gammon, a self-teaching backgammon program, achieves master-level play. Neural computation, 1994.
- Tomar, M., Shani, L., Efroni, Y., and Ghavamzadeh, M. Mirror descent policy optimization, 2021.

- van Hasselt, H., Doron, Y., Strub, F., Hessel, M., Sonnerat, N., and Modayil, J. Deep reinforcement learning and the deadly triad. [arXiv](#), 2018.
- van Seijen, H., Fatemi, M., and Tavakoli, A. Using a logarithmic mapping to enable lower discount factors in reinforcement learning. *Advances in Neural Information Processing Systems*, 2019.
- Wang, Y., He, H., Tan, X., and Gan, Y. Trust region-guided proximal policy optimization. In *Advances in Neural Information Processing Systems*, 2019.
- Wang, Z., Schaul, T., Hessel, M., Hasselt, H., Lanctot, M., and Freitas, N. Dueling network architectures for deep reinforcement learning. In *International conference on machine learning*, pp. 1995–2003. PMLR, 2016.
- Watkins, C. J. and Dayan, P. Q-learning. *Machine learning*, 1992.
- Williams, J. D., Asadi, K., and Zweig, G. Hybrid code networks: practical and efficient end-to-end dialog control with supervised and reinforcement learning. In *Association for Computational Linguistics*, 2017.
- Zhang, S., Yao, H., and Whiteson, S. Breaking the deadly triad with a target network. [arXiv](#), 2021.

9. Appendix

9.1. Implementation Details

Table 1 and 2 show hyper-parameters, computing infrastructure, and libraries used for the experiments in this paper for all games tested. Our training and evaluation protocols and the hyper-parameter settings closely follow those of the Dopamine baseline. To report performance results, we measured the undiscounted sum of rewards obtained by the learned policy during evaluation.

DQN and DDQN hyper-parameters (shared)	
Replay buffer size	200000
Target update period	8000
Max steps per episode	27000
Evaluation frequency	10000
Batch size	64
Update period	4
Number of frame skip	4
Number of episodes to evaluate	2
Update horizon	1
ϵ -greedy (training time)	0.01
ϵ -greedy (evaluation time)	0.001
ϵ -greedy decay period	250000
Burn-in period / Min replay size	20000
Learning rate	10^{-4}
Discount factor (γ)	0.99
Total number of iterations	3×10^7
Sticky actions	True
Optimizer	Adam (Kingma & Ba, 2015)
Network architecture	Nature DQN network (Mnih et al., 2015)
Random seeds	{0, 1, 2, 3, 4}
Rainbow hyper-parameters (shared)	
Batch size	64
Other	Config file rainbow_aaai.gin from Dopamine
DQN Pro and Rainbow Pro hyper-parameter	
\tilde{c} (DQN Pro)	0.2
\tilde{c} (Rainbow Pro)	0.05

Table 1. Hyper-parameters used for all methods for all 55 games of Atari-2600 benchmarks

. All results reported in our paper are averages over repeated runs initialized with each of the random seeds listed above and run for the listed number of episodes.

Computing Infrastructure	
Machine Type	AWS EC2 - p2.16xlarge
GPU Family	Tesla K80
CPU Family	Intel Xeon 2.30GHz
CUDA Version	11.0
NVIDIA-Driver	450.80.02
Library Version	
Python	3.8.5
Numpy	1.20.1
Gym	0.18.0
Pytorch	1.8.0

Table 2. Computing infrastructure and software libraries used in all experiments in this paper.

9.2. Proofs

Theorem 1. *The Proximal Bellman Optimality Operator $\mathcal{T}_{c,f}^*$ is a contraction with fixed point v^* .*

We make two assumptions:

1. f is smooth, or more specifically that its gradient is 1-Lipschitz: $\|\nabla f(v_1) - \nabla f(v_2)\| \leq \|v_1 - v_2\| \forall v_1, \forall v_2$.
2. the value of the parameter c is large, in particular $c > \frac{2}{1-\gamma}$.

Proof. Both terms are convex and differentiable, therefore by setting the gradient to zero, we have:

$$\mathcal{T}_{c,f}^* v = T^* v + \frac{1}{c} (\nabla f(v) - \nabla f(\mathcal{T}_{c,f}^* v)),$$

We can then show:

$$\begin{aligned} \|\mathcal{T}_{c,f}^* v_1 - \mathcal{T}_{c,f}^* v_2\| &= \|T^* v_1 + \frac{1}{c} (\nabla f(v_1) - \nabla f(\mathcal{T}_{c,f}^* v_1)) - T^* v_2 - \frac{1}{c} (\nabla f(v_2) - \nabla f(\mathcal{T}_{c,f}^* v_2))\| \\ &\leq \|T^* v_1 - T^* v_2\| + \frac{1}{c} \|\nabla f(v_1) - \nabla f(v_2)\| + \frac{1}{c} \|\nabla f(\mathcal{T}_{c,f}^* v_1) - \nabla f(\mathcal{T}_{c,f}^* v_2)\| \\ &\quad \text{(first assumption)} \\ &\leq \|T^* v_1 - T^* v_2\| + \frac{1}{c} \|\nabla f(v_1) - \nabla f(v_2)\| + \frac{1}{c} \|\mathcal{T}_{c,f}^* v_1 - \mathcal{T}_{c,f}^* v_2\| \end{aligned}$$

This implies:

$$\begin{aligned} \frac{c-1}{c} \|\mathcal{T}_{c,f}^* v_1 - \mathcal{T}_{c,f}^* v_2\| &\leq \|T^* v_1 - T^* v_2\| + \frac{1}{c} \|\nabla f(v_1) - \nabla f(v_2)\| \\ &\quad \text{(first assumption)} \\ &\leq \|T^* v_1 - T^* v_2\| + \frac{1}{c} \|v_1 - v_2\| \\ &\leq \frac{\gamma c + 1}{c} \|v_1 - v_2\| \end{aligned}$$

Therefore,

$$\|\mathcal{T}_{c,f}^* v_1 - \mathcal{T}_{c,f}^* v_2\| \leq \frac{\gamma c + 1}{c - 1} \|v_1 - v_2\|,$$

Allowing us to conclude that $\mathcal{T}_{c,f}^*$ is a contraction (second assumption).

Further, to show that v^* is indeed the fixed point of $\mathcal{T}_{c,f}^*$, notice from the original formulation:

$$\mathcal{T}_{c,f}^* v := \arg \min_{v'} \|v' - T^* v\|_2^2 + \frac{1}{c} D_f(v', v),$$

that, at point v^* setting $v' = v^*$ jointly minimizes the first term, because $v^* = \mathcal{T}^* v^*$ due to fixed-point definition, and it also minimizes the second term because $D_f(v^*, v^*) = 0$ and that Bregman divergence is non-negative. Therefore, $\mathcal{T}_{c,f}^* v^* = v^*$; v^* is the fixed-point of $\mathcal{T}_{c,f}^*$. Since, $\mathcal{T}_{c,f}^*$ is a contraction, this fixed point is unique. \square

Theorem 2. Consider the PMPI algorithm specified by:

$$\pi_k \leftarrow \mathcal{G}_{\epsilon'_k} v_{k-1}, \quad (4)$$

$$v_k \leftarrow (\mathcal{T}_\beta^{\pi_k})^n v_{k-1} + (1 - \beta)\epsilon_k. \quad (5)$$

Define the Bellman residual $b_k := v_k - \mathcal{T}^{\pi_{k+1}} v_k$, and error terms $x_k := (I - \gamma P^{\pi_k})\epsilon_k$ and $y_k := \gamma P^{\pi^*} \epsilon_k$. After k steps:

$$v^* - v^{\pi_k} = \underbrace{v^{\pi^*} - (\mathcal{T}_\beta^{\pi_{k+1}})^n v_k}_{d_k} + \underbrace{(\mathcal{T}_\beta^{\pi_{k+1}})^n v_k - v_{\pi_k}}_{s_k}$$

- where $d_k \leq \gamma P^{\pi^*} d_{k-1} - ((1 - \beta)y_{k-1} + \beta b_{k-1}) + (1 - \beta) \sum_{j=1}^{n-1} (\gamma P^{\pi_k})^j b_{k-1} + \epsilon'_k$
- $s_k \leq ((1 - \beta)(\gamma P^{\pi_k})^n + \beta I)(I - \gamma P^{\pi_k})^{-1} b_{k-1}$
- $b_k \leq ((1 - \beta)(\gamma P^{\pi_k})^n + \beta I)b_{k-1} + (1 - \beta)x_k + \epsilon'_{k+1}$

We make two assumptions:

1. we assume ϵ error in policy evaluation step, as already stated in equation (4).
2. we assume ϵ' error in policy greedification step $\pi_k \leftarrow \mathcal{G}_{\epsilon'_k} v_{k-1} \forall k$. This means $\forall \pi \mathcal{T}^\pi v_k - \mathcal{T}^{\pi_{k+1}} v_k \leq \epsilon'_{k+1}$. Note that this assumption is orthogonal to the thesis of our paper, but we kept it for generality.

Proof. Step 0: bound the Bellman residual: $b_k := v_k - \mathcal{T}^{\pi_{k+1}} v_k$.

$$\begin{aligned} b_k &= v_k - \mathcal{T}^{\pi_{k+1}} v_k \\ &= v_k - \mathcal{T}^{\pi_k} v_k + \mathcal{T}^{\pi_k} v_k - \mathcal{T}^{\pi_{k+1}} v_k \\ &\quad (\text{from our assumption } \forall \pi \mathcal{T}^\pi v_k - \mathcal{T}^{\pi_{k+1}} v_k \leq \epsilon'_{k+1}) \\ &\leq v_k - \mathcal{T}^{\pi_k} v_k + \epsilon'_{k+1} \\ &= v_k - (1 - \beta)\epsilon_k - \mathcal{T}^{\pi_k} v_k + (1 - \beta)\gamma P^{\pi_k} \epsilon_k + (1 - \beta)\epsilon_k - (1 - \beta)\gamma P^{\pi_k} \epsilon_k + \epsilon'_{k+1} \\ &\quad \left(\text{from } \mathcal{T}^{\pi_k} v_k + (1 - \beta)\gamma P^{\pi_k} \epsilon_k = \mathcal{T}^{\pi_k} (v_k - (1 - \beta)\epsilon_k) \right) \\ &= v_k - (1 - \beta)\epsilon_k - \mathcal{T}^{\pi_k} (v_k - (1 - \beta)\epsilon_k) + (1 - \beta) \underbrace{(I - \gamma P_{\pi_k})\epsilon_k}_{x_k} + \epsilon'_{k+1} \\ &= v_k - (1 - \beta)\epsilon_k - \mathcal{T}^{\pi_k} (v_k - (1 - \beta)\epsilon_k) + (1 - \beta)x_k + \epsilon'_{k+1} \\ &\quad (\text{from } v_k - (1 - \beta)\epsilon_k = (\mathcal{T}_\beta^{\pi_k})^n v_{k-1}) \\ &= (1 - \beta)(\mathcal{T}^{\pi_k})^n v_{k-1} + \beta v_{k-1} - \mathcal{T}^{\pi_k} ((1 - \beta)(\mathcal{T}^{\pi_k})^n v_{k-1} + \beta v_{k-1}) + (1 - \beta)x_k + \epsilon'_{k+1} \\ &\quad (\text{from linearity of } \mathcal{T}^{\pi_k}) \\ &= (1 - \beta)(\mathcal{T}^{\pi_k})^n v_{k-1} - \mathcal{T}^{\pi_k} ((1 - \beta)(\mathcal{T}^{\pi_k})^n v_{k-1}) + \beta(v_{k-1} - \mathcal{T}^{\pi_k} v_{k-1}) + (1 - \beta)x_k + \epsilon'_{k+1} \\ &= (1 - \beta) \left((\mathcal{T}^{\pi_k})^n v_{k-1} - \mathcal{T}^{\pi_k} ((\mathcal{T}^{\pi_k})^n v_{k-1}) \right) + \beta(v_{k-1} - \mathcal{T}^{\pi_k} v_{k-1}) + (1 - \beta)x_k + \epsilon'_{k+1} \\ &= (1 - \beta) \left((\mathcal{T}^{\pi_k})^n v_{k-1} - (\mathcal{T}^{\pi_k})^n (\mathcal{T}^{\pi_k} v_{k-1}) \right) + \beta(v_{k-1} - \mathcal{T}^{\pi_k} v_{k-1}) + (1 - \beta)x_k + \epsilon'_{k+1} \\ &= (1 - \beta) \underbrace{(\gamma P^{\pi_k})^n (v_{k-1} - \mathcal{T}^{\pi_k} (v_{k-1}))}_{=b_{k-1}} + \beta \underbrace{(v_{k-1} - \mathcal{T}^{\pi_k} v_{k-1})}_{=b_{k-1}} + (1 - \beta)x_k + \epsilon'_{k+1}, \end{aligned}$$

allowing us to conclude:

$$b_k = ((1 - \beta)(\gamma P^{\pi_k})^n + \beta I)b_{k-1} + (1 - \beta)x_k + \epsilon'_{k+1}.$$

Step 1: bound the distance to the optimal value: $d_{k+1} := v^* - (\mathcal{T}_\beta^{\pi_{k+1}})^n v_k$.

$$\begin{aligned}
 d_{k+1} &= v^* - (\mathcal{T}_\beta^{\pi_{k+1}})^n v_k \\
 &= \mathcal{T}^{\pi^*} v^* - \mathcal{T}^{\pi^*} v_k + \underbrace{\mathcal{T}^{\pi^*} v_k - \mathcal{T}^{\pi_{k+1}} v_k}_{\leq \epsilon'_{k+1}} + \underbrace{\mathcal{T}^{\pi_{k+1}} v_k - (\mathcal{T}_\beta^{\pi_{k+1}})^n v_k}_{=g_{k+1}} \\
 &\leq \gamma P^{\pi^*} (v^* - v_k) + \epsilon'_{k+1} + g_{k+1} \\
 &= \gamma P^{\pi^*} (v^* - v_k) + (1 - \beta) \gamma P^{\pi^*} \epsilon_k - (1 - \beta) \gamma P^{\pi^*} \epsilon_k + \epsilon'_{k+1} + g_{k+1} \\
 &= \gamma P^{\pi^*} (v^* - (v_k - (1 - \beta) \epsilon_k)) - (1 - \beta) \underbrace{\gamma P^{\pi^*} \epsilon_k}_{y_k} + \epsilon'_{k+1} + g_{k+1} \\
 &= \gamma P^{\pi^*} (\underbrace{v^* - (\mathcal{T}_\beta^{\pi_k})^n v_{k-1}}_{=d_k}) - (1 - \beta) y_k + \epsilon'_{k+1} + g_{k+1} \\
 &= \gamma P^{\pi^*} d_k - (1 - \beta) y_k + \epsilon'_{k+1} + g_{k+1}
 \end{aligned}$$

Additionally we can bound g_{k+1} as follows:

$$\begin{aligned}
 g_{k+1} &= \mathcal{T}^{\pi_{k+1}} v_k - (\mathcal{T}_\beta^{\pi_{k+1}})^n v_k \\
 &= (1 - \beta) (\mathcal{T}^{\pi_{k+1}} v_k - (\mathcal{T}^{\pi_{k+1}})^n v_k) + \beta (\mathcal{T}^{\pi_{k+1}} v_k - v_k) \\
 &= (1 - \beta) \sum_{j=1}^{n-1} (\gamma P^{\pi_{k+1}})^j b_k + \beta (-b_k)
 \end{aligned}$$

Allowing us to conclude that:

$$d_{k+1} \leq \gamma P^{\pi^*} d_k - ((1 - \beta) y_k + \beta b_k) + (1 - \beta) \sum_{j=1}^{n-1} (\gamma P^{\pi_{k+1}})^j b_k + \epsilon'_{k+1}$$

Step 2: bound the distance between the approximate value and the value of the policy: $s_k := (\mathcal{T}_\beta^{\pi_k})^n v_{k-1} - v^{\pi_k}$.

$$\begin{aligned}
 s_k &= (\mathcal{T}_\beta^{\pi_k})^n v_{k-1} - v^{\pi_k} \\
 &= (\mathcal{T}_\beta^{\pi_k})^n v_{k-1} - (\mathcal{T}^{\pi_k})^\infty v_{k-1} \\
 &= (1 - \beta) (\mathcal{T}^{\pi_k})^n v_{k-1} + \beta v_{k-1} - (1 - \beta) (\mathcal{T}^{\pi_k})^\infty v_{k-1} - \beta (\mathcal{T}^{\pi_k})^\infty v_{k-1} \\
 &= (1 - \beta) ((\mathcal{T}^{\pi_k})^n v_{k-1} - (\mathcal{T}^{\pi_k})^\infty v_{k-1}) + \beta (v_{k-1} - (\mathcal{T}^{\pi_k})^\infty v_{k-1}) \\
 &= (1 - \beta) (\gamma P^{\pi_k})^n (v_{k-1} - (\mathcal{T}^{\pi_k})^\infty v_{k-1}) + \beta (v_{k-1} - (\mathcal{T}^{\pi_k})^\infty v_{k-1}) \\
 &= ((1 - \beta) (\gamma P^{\pi_k})^n + \beta I) (v_{k-1} - (\mathcal{T}^{\pi_k})^\infty v_{k-1}) \\
 &= ((1 - \beta) (\gamma P^{\pi_k})^n + \beta I) (I - \gamma P^{\pi_k})^{-1} (\underbrace{v_{k-1} - \mathcal{T}^{\pi_k} v_{k-1}}_{b_{k-1}}).
 \end{aligned}$$

Allowing us to conclude that:

$$s_k = ((1 - \beta) (\gamma P^{\pi_k})^n + \beta I) (I - \gamma P^{\pi_k})^{-1} b_{k-1}.$$

□

10. Learning curves

Below, we present full learning curves of DQN, DQN Pro, Rainbow, and Rainbow Pro for the 55 Atari games.

Proximal Iteration for Deep Reinforcement Lefarning

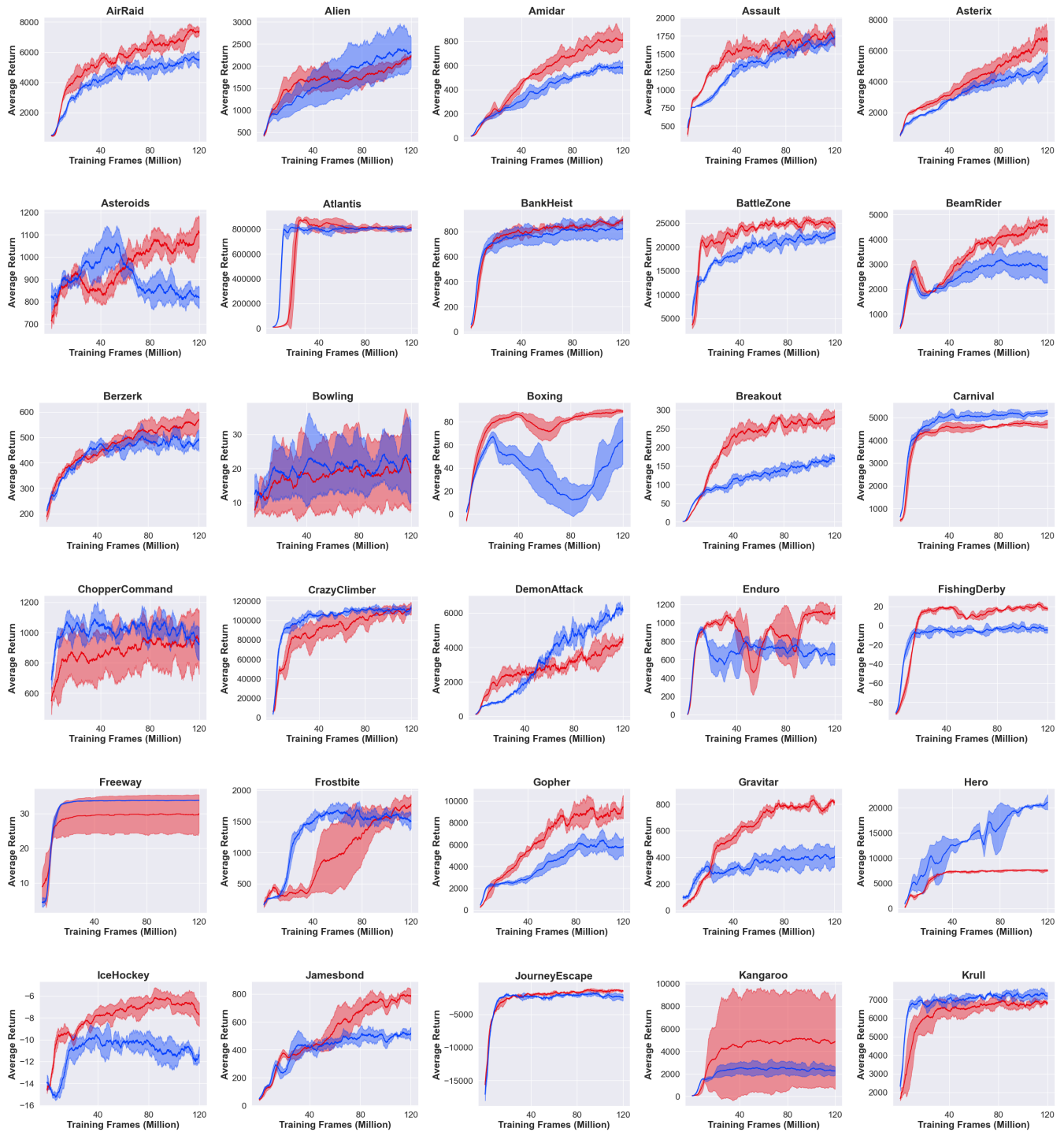


Figure 7. Comparison between DQN Pro (red) and DQN (blue) over 55 Atari games (Part I).

Proximal Iteration for Deep Reinforcement Lefarning

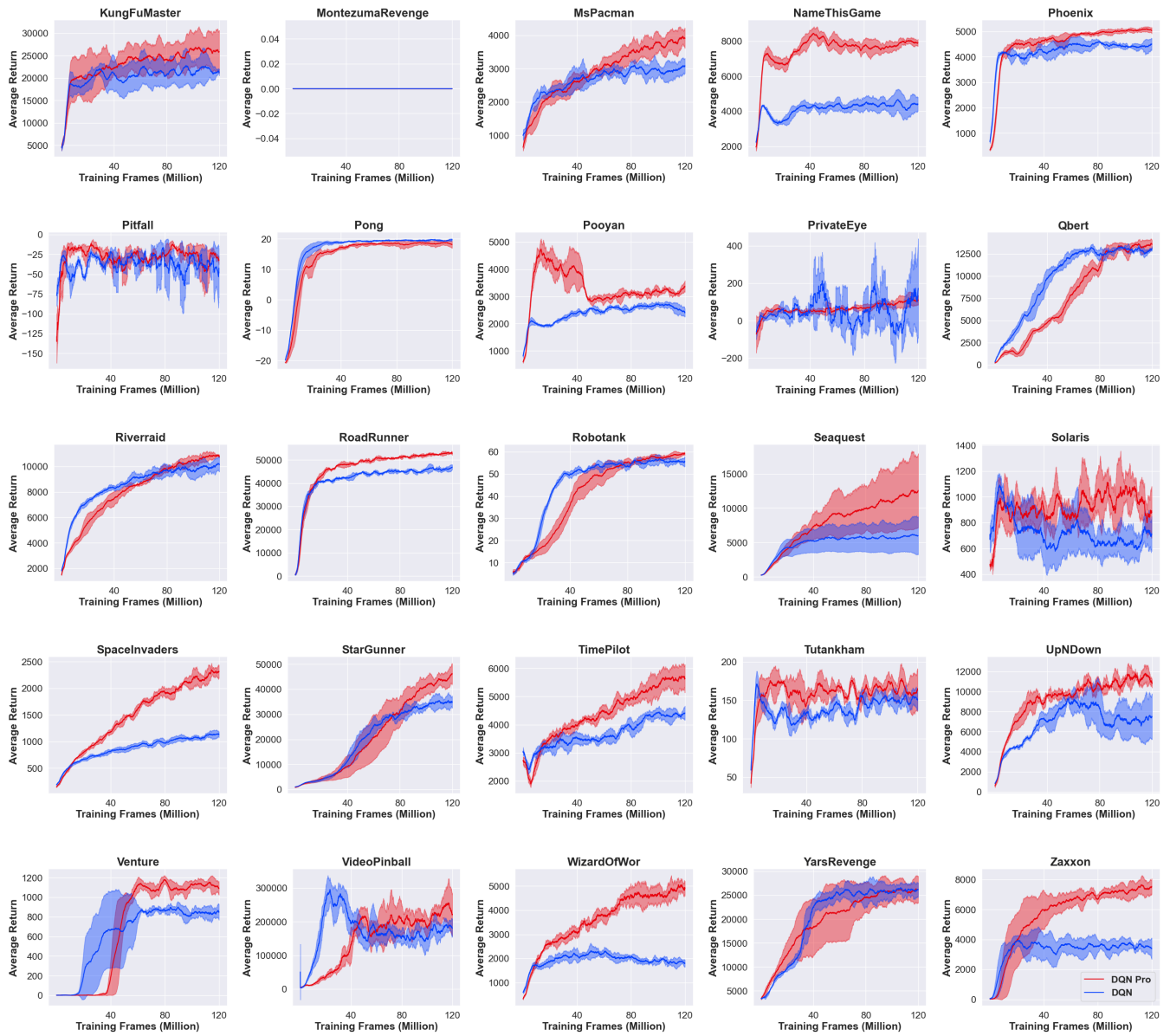


Figure 8. Comparison between DQN Pro (red) and DQN (blue) over 55 Atari games (Part II).

Proximal Iteration for Deep Reinforcement Lefarning

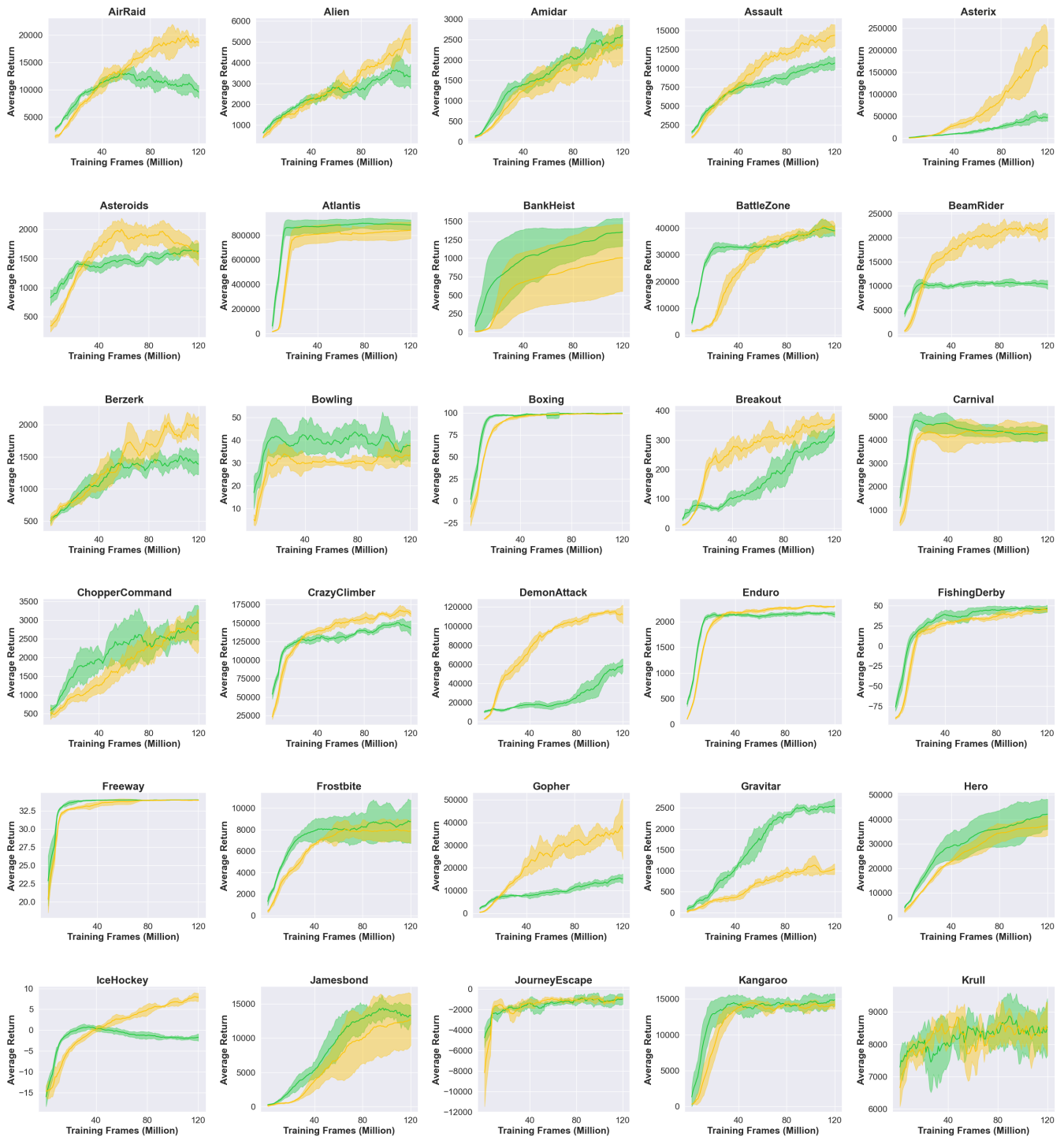


Figure 9. Comparison between Rainbow Pro (yellow) and Rainbow (green) over 55 Atari games (Part I).

Proximal Iteration for Deep Reinforcement Lefarning

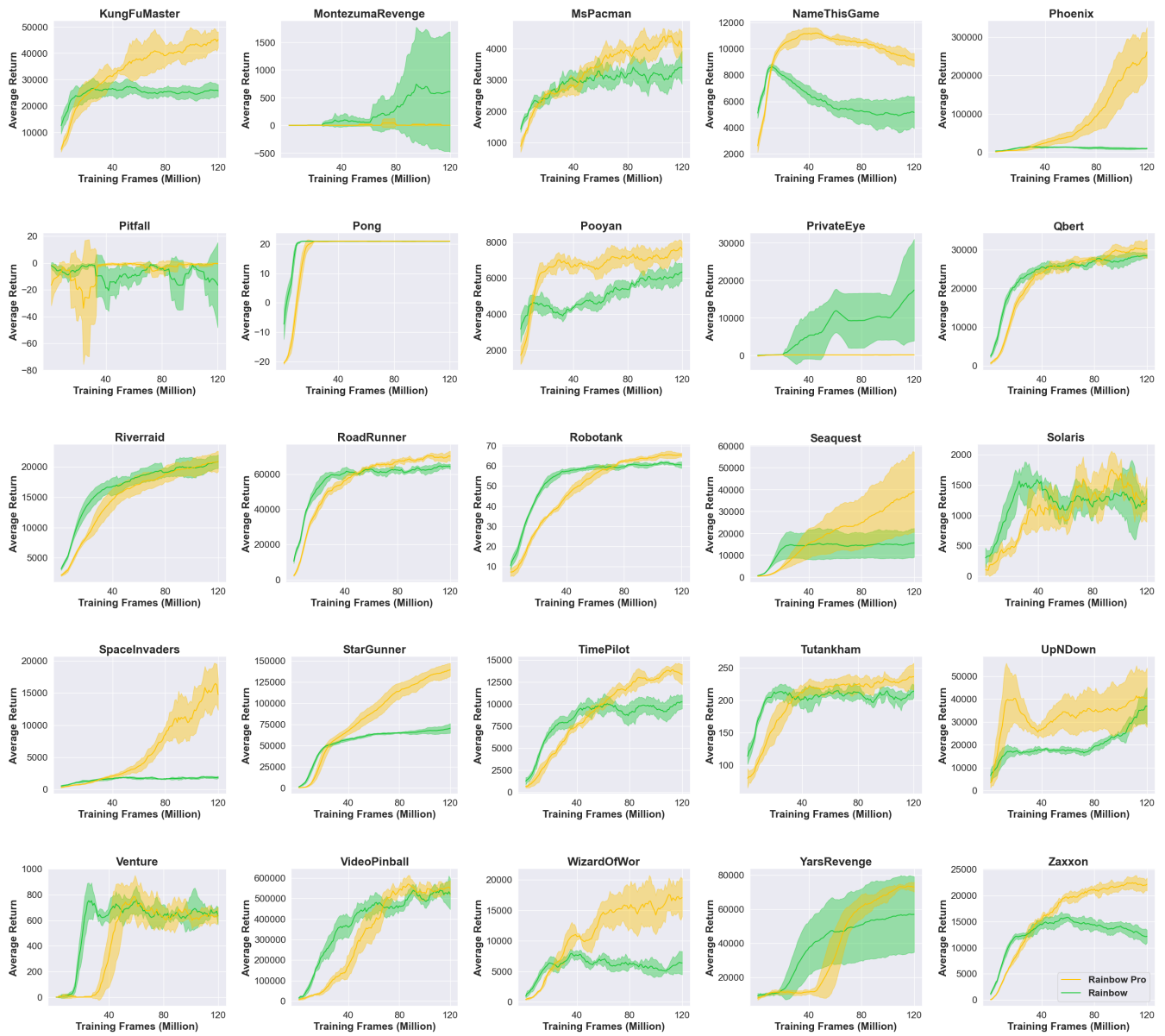


Figure 10. Comparison between Rainbow Pro (yellow) and Rainbow (green) over 55 Atari games (Part II).